Supplementary Information (SI) for New Journal of Chemistry.

Supporting Information

Perylene functionalized Fluorescent Zirconium based Metal Organic Frameworks for selective sensing of Cu^{2+}, Pb^{2+}, and Fe^{3+} ions

Arumugam Santhana Mariappan[a], Kettalu Ananthan Karthick[b], Tamilselvi Arunachalam[b]

Bhaskaran Shankar[a*]

[a]Functional Materials Laboratory, Department of Chemistry, Thiagarajar College of Engineering, Madurai, Tamil Nadu, India-625 015.

E-mail: bshankardu@gmail.com, bsrchem@tce.edu

[b]PG & Research Department of Chemistry, Thiagarajar College, Madurai, Tamilnadu, India-625 009.

Table of contents

11.	**Fig. S10** Determination of LOD (a) Linear regressive plot of UiO-66-NH-PTCDA-Na with Cu^{2+} ion concentration (b) Linear regressive plot of UiO-66-NH-PTCDA-Na with Pb^{2+} ion concentration (c) Linear regressive plot of UiO-66-NH-PTCDA-Na with Fe^{3+} ion concentration.	**SI 11**
12.	**Fig. S11.** Fluorescence interference study of UiO-66-NH-PTCDA-Na in the presence of competitive metal ions (1 equiv.) with and without Cu^{2+} ions (1.0 equiv.)	**SI 12**
13.	**Fig. S12.** Fluorescence interference study of UiO-66-NH-PTCDA-Na in the presence of competitive metal ions (1 equiv.) with and without Fe^{3+} ions (1.0 equiv.)	**SI 12**
14.	**Fig. S13.** Fluorescence interference study of UiO-66-NH-PTCDA-Na in the presence of competitive metal ions (1 equiv.) with and without Pb^{2+} ions (1.0 equiv.)	**SI 13**
15.	**Fig. S14.** FT-IR spectra of UiO-66-NH-PTCDA-Na in the presence and absence of sensing metal ions (Cu^{2+}, Fe^{3+} & Pb^{2+}).	**SI 13**
16.	**Table S1.** The changing of Fluorescence maxima (λ_{ex} = 440 nm) of UiO-66-NH-PTCDA-Na corresponding to pH ranges.	**SI 7**
17.	**Table S2.** Comparison of fluorescence sensing performance of UiO-66-NH_2 based MOFs with literature.	**SI 14**

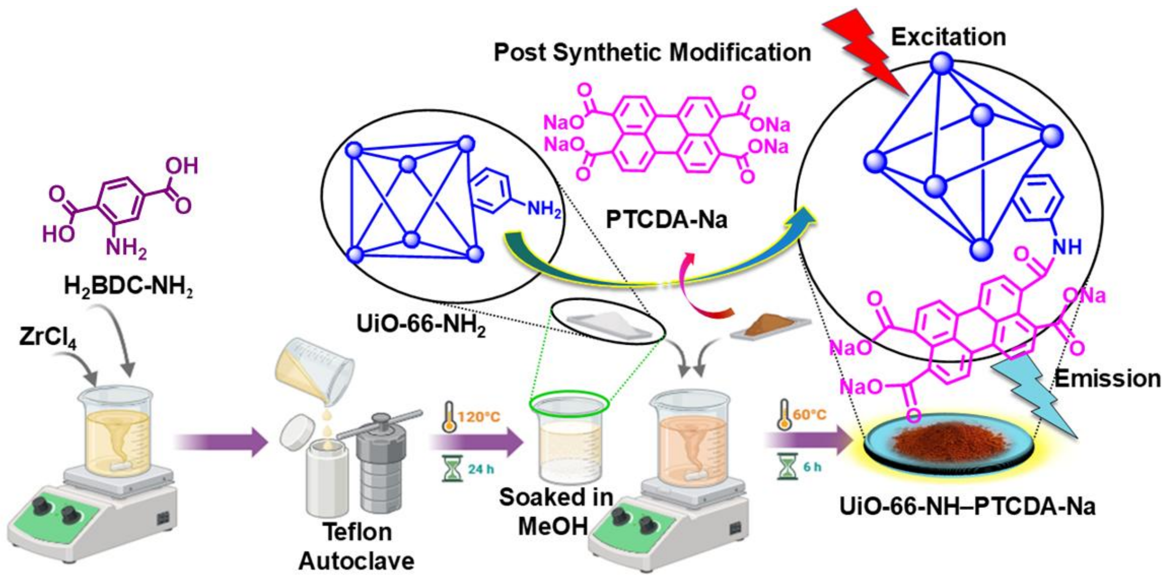

Scheme S1. Synthetic route of Post synthetic modification of UiO-66-NH_2 using PTCDA-Na.

Determination of optical band gap (UV-DRS) study

The fine powdered samples of UiO-66-NH_2, PTCDA-Na and UiO-66-NH-PTCDA-Na were carefully filled with solid sample cell holder. The correlation between absorption co-efficient (α) and optical band gap (E_g) is given by the equation (1),

$$\boldsymbol{\alpha E \approx A_1(E - E_g)^2} \qquad \text{.....(1)}$$

Where, $E = h\nu$ is photon energy, A_1 is a constant

Kubelka-Munk (K-M) equation (2) is given by,

$$\boldsymbol{F(R) = \frac{(1 - R^2)}{2R} = \frac{k}{s}} \qquad \text{.....(2)}$$

Where, R is experimentally observed reflectance, k is molar absorption co-efficient and s is scattering co-efficient. The scattering co-efficient is independent on the wavelength of incident light and using equation (1) & (2), the following equation (3) can be written as follows,

$$\boldsymbol{[h\nu F(R)]^2 = A_1[h\nu - E_g]} \qquad \text{.....(3)}$$

The plot Kubelka-Munk (K-M) function $[h\nu F(R)]^2$ versus photon energy is known as Tauc plot[1,2]. The optical band gap energy (E_g) of UiO-66-NH_2, PTCDA-Na and UiO-66-NH-PTCDA-Na were determined by extrapolating the linear fitted region to $[h\nu F(R)]^{1/2} = 0$.

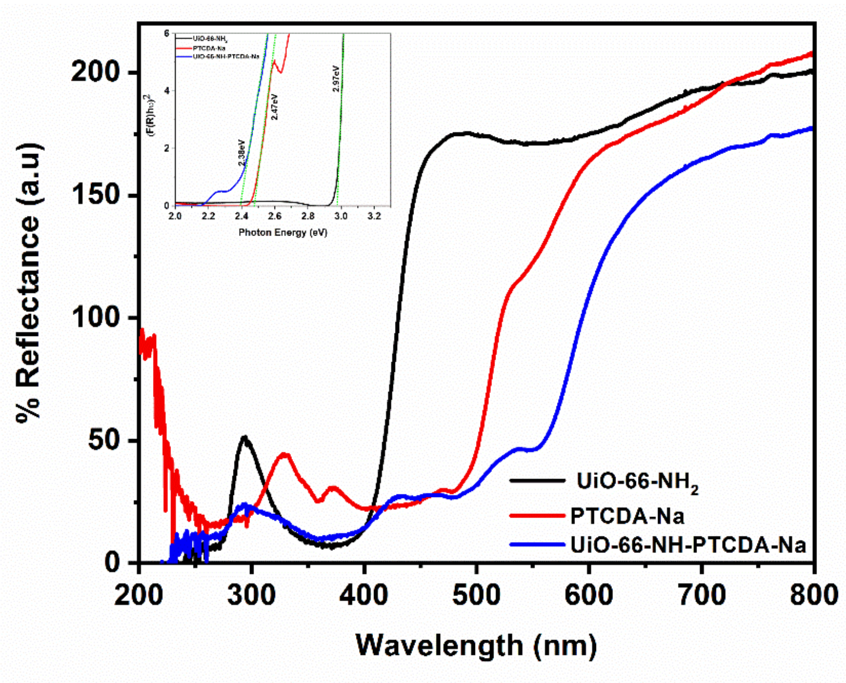

Fig. S1 UV-DRS plot of UiO-66-NH_2, PTCDA-Na and UiO-66-NH-PTCDA-Na, Inset; Kubulka-Munk plot[1] used for determination of optical band gap.

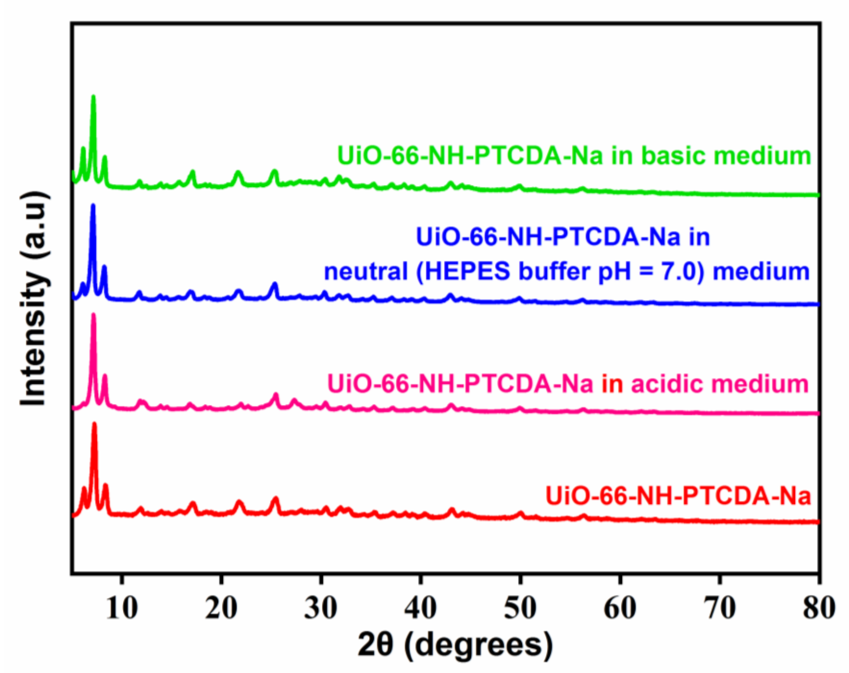

Fig. S2. PXRD pattern of UiO-66-NH-PTCDA-Na under acidic, basic and HEPES (pH = 7.0) medium.

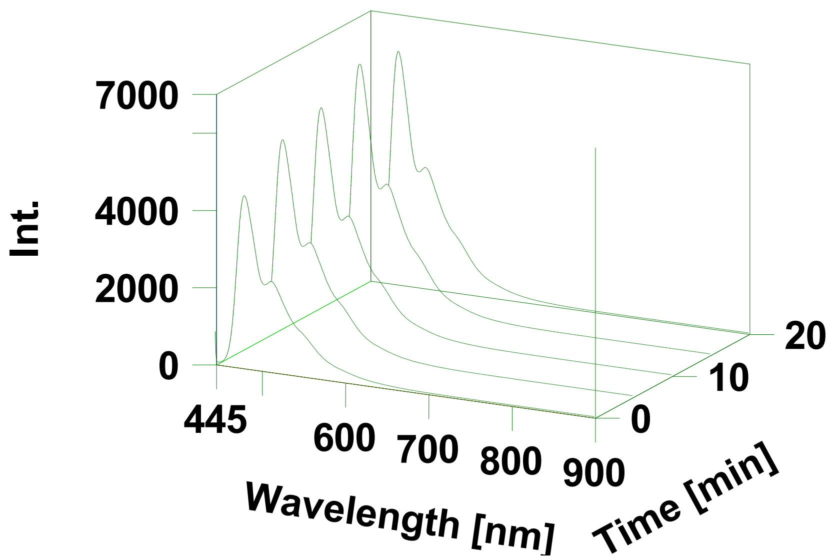

Fig. S3. Interval scan time course measurement study of UiO-66-NH-PTCDA-Na

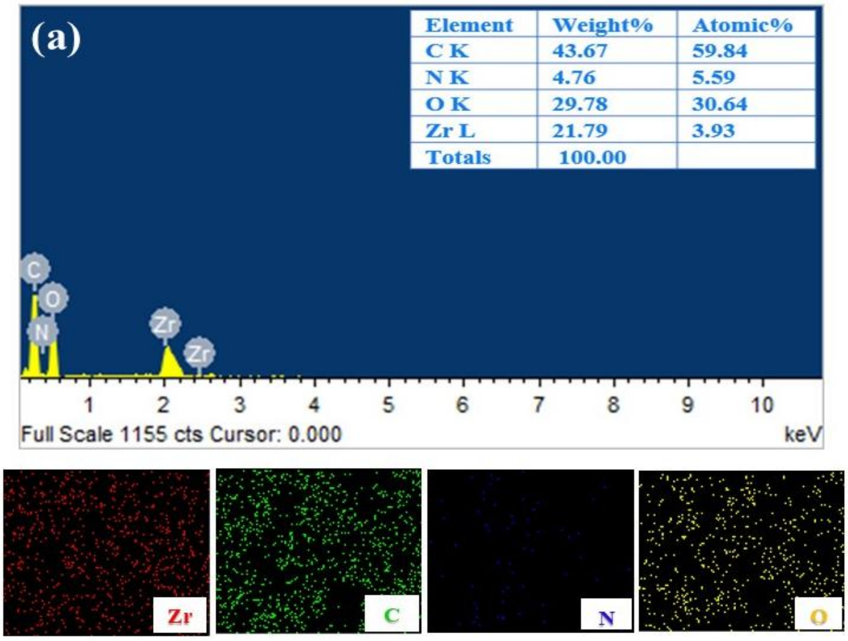
(a)
Element Weight% Atomic%
C K 43.67 59.84
N K 4.76 5.59
O K 29.78 30.64
Zr L 21.79 3.93
Totals 100.00
C
O
N
Zr
Zr
1 2 3 4 5 6 7 8 9 10
Full Scale 1155 cts Cursor: 0.000
keV
Zr
C
N
O

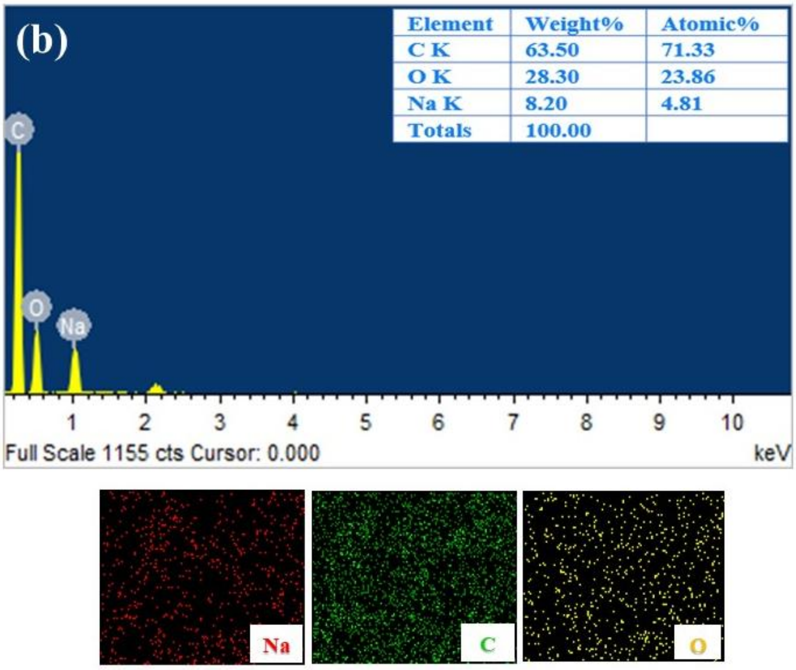
(b)
Element Weight% Atomic%
C K 63.50 71.33
O K 28.30 23.86
Na K 8.20 4.81
Totals 100.00
C
O
Na
1 2 3 4 5 6 7 8 9 10
Full Scale 1155 cts Cursor: 0.000
keV
Na
C
O

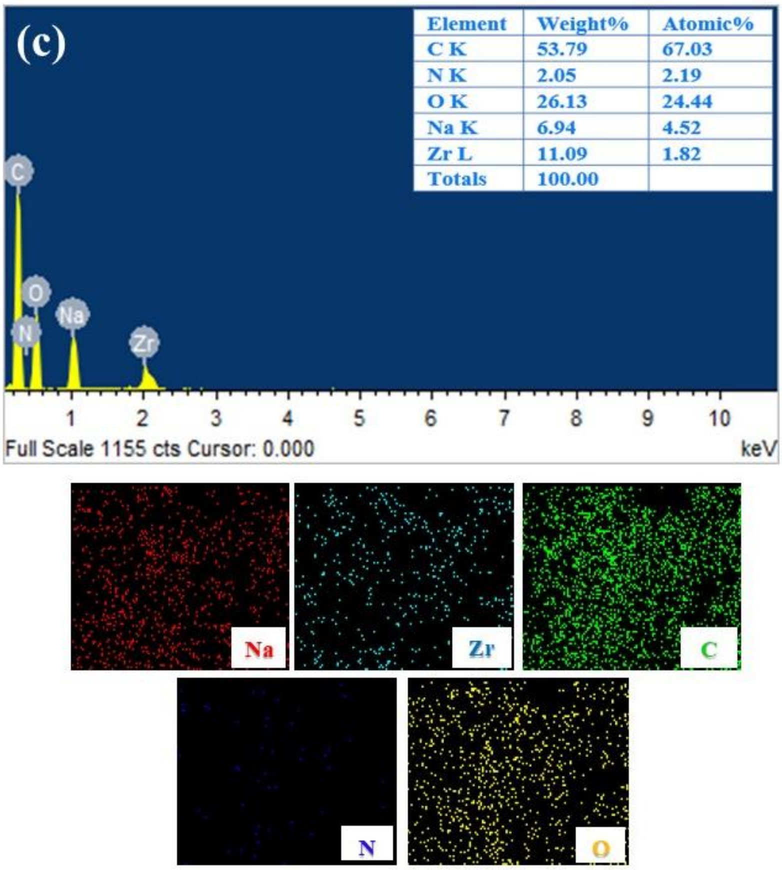

Fig. S4 EDX spectrum and elemental distribution of UiO-66-NH_2, PTCDA-Na and UiO-66-NH-PTCDA-Na

Table S1. The changing of Fluorescence maxima (λ_{ex} = 440 nm) of UiO-66-NH-PTCDA-Na corresponding to pH ranges.

pH	3.0	4.0	5.0	6.0	7.0	8.0	9.0	10.0
λ_{emi} (nm)	491	491	491	484	479	478	479	479
	529	529	527	514	514	511	514	512

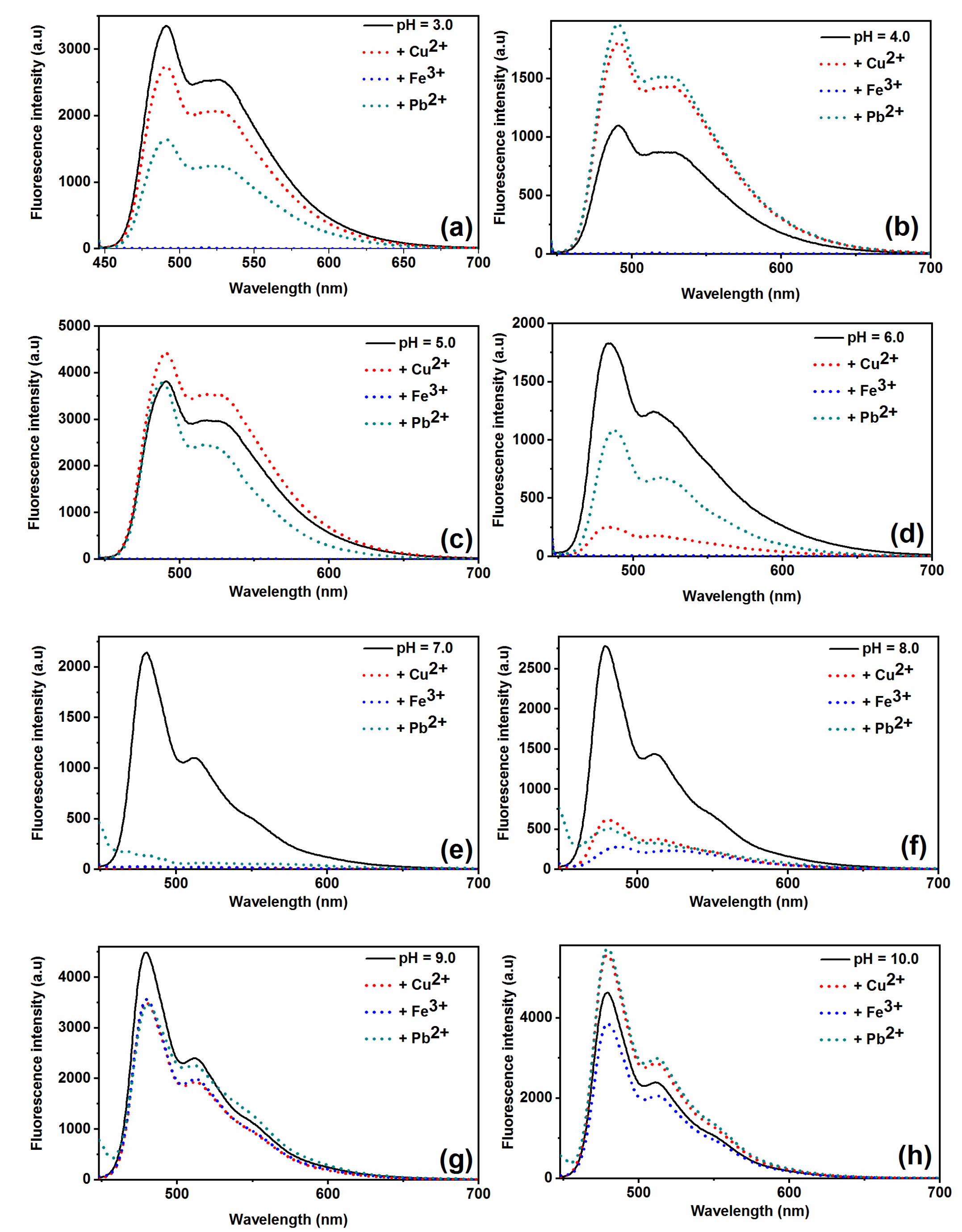

Fig. S5 Effect of pH on Fluorescence quenching effect of UiO-66-NH-PTCDA-Na in the presence and absence of sensing metal ions (Cu^{2+}, Fe^{3+} & Pb^{2+})

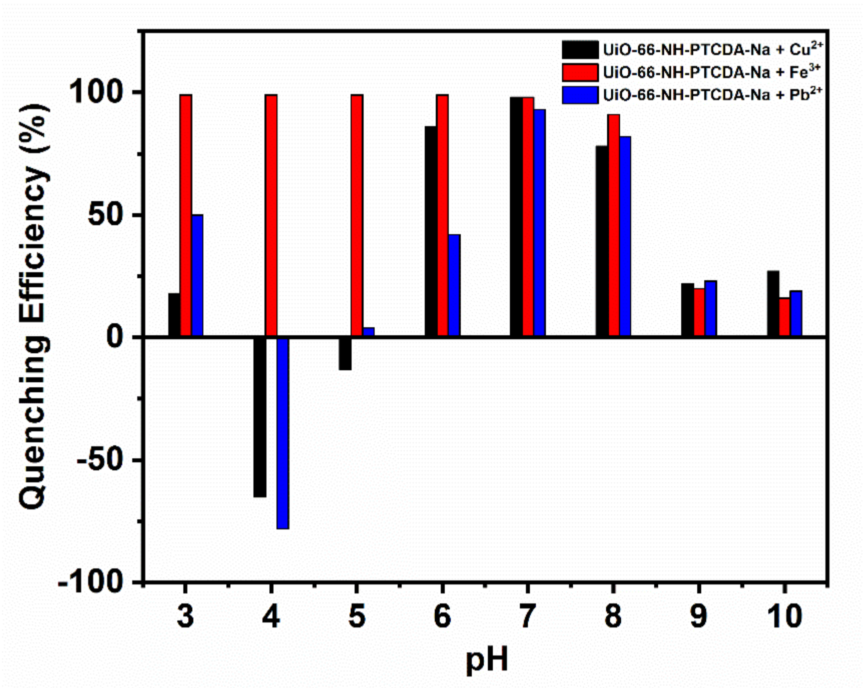

Fig. S6 Effect of pH on quenching efficiency of UiO-66-NH-PTCDA-Na for sensing metal ions.

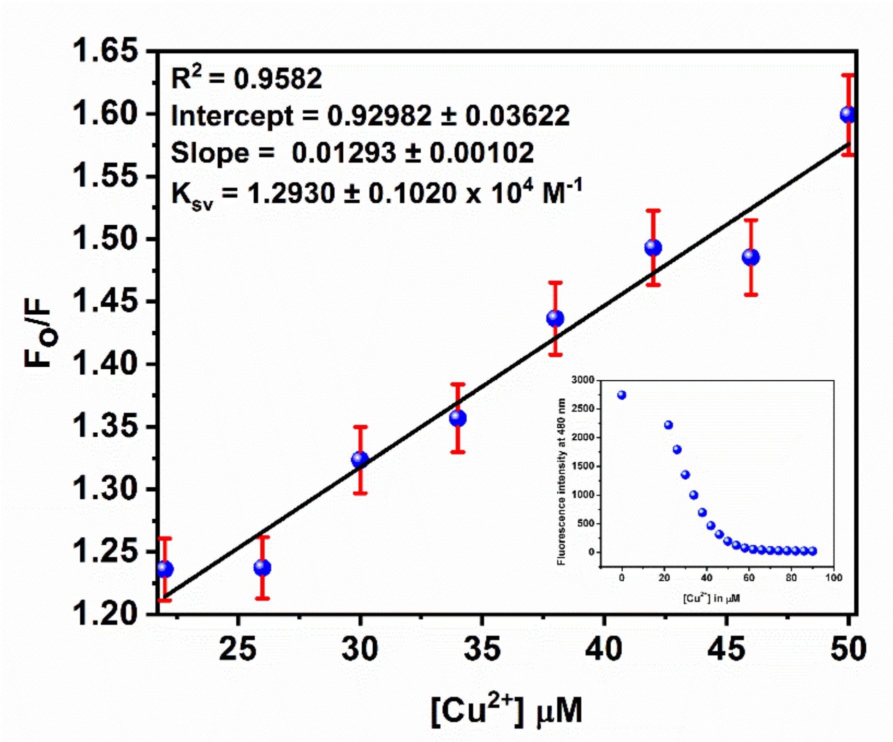

Fig. S7 Stern-Volmer plot of fluorescence changes at 480 nm upon addition of Cu^{2+} ion (linearity plotted using the addition from 22 μM to 50 μM of Cu^{2+} to UiO-66-NH-PTCDA-Na); inset: Non-linear quenching response of UiO-66-NH-PTCDA-Na with sequence addition of Cu^{2+} ions (22 to 90 μM).

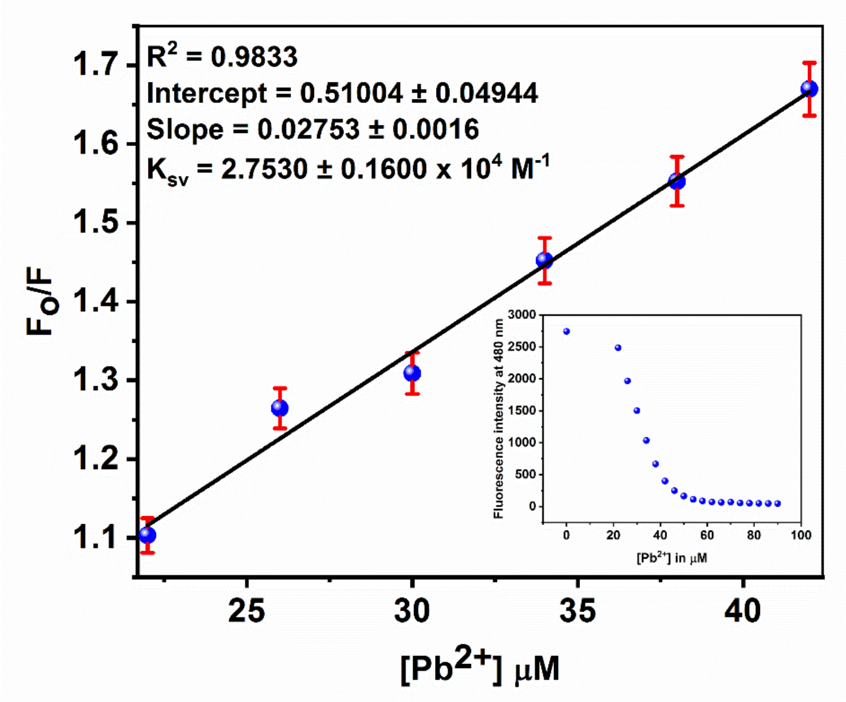

Fig. S8 Stern-Volmer plot of fluorescence changes at 480 nm upon addition of Pb^{2+} ion (linearity plotted using the addition from 22 μM to 50 μM of Pb^{2+} to UiO-66-NH-PTCDA-Na); Inset: Non-linear quenching response of UiO-66-NH-PTCDA-Na with sequence addition of Pb^{2+} ions (22 to 90 μM).

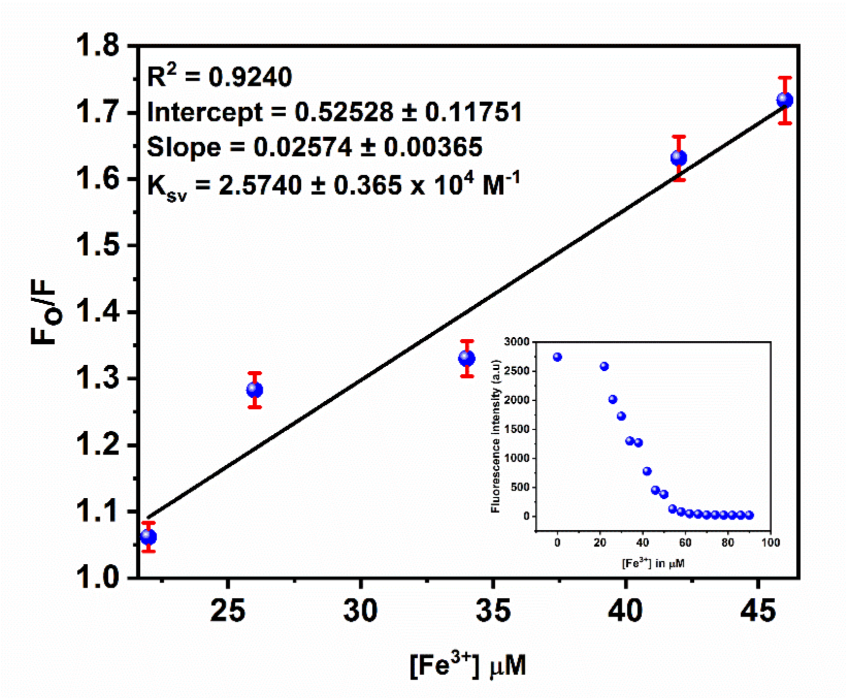

Fig. S9 Stern-Volmer plot of fluorescence changes at 480 nm upon addition of Fe^{3+} ion (linearity plotted using the addition from 22 μM to 42 μM of Fe^{3+} to UiO-66-NH-PTCDA-Na);

Inset: Non-linear quenching response of UiO-66-NH-PTCDA-Na with sequence addition of Fe^{3+} ions (22 to 90 μM).

Determination of Limit of Detection (LOD)

The limit of detection (LOD) was determined using following formula,

$$\mathbf{LOD} = \frac{\mathbf{3\sigma}}{\mathbf{k}} \qquad \text{.....(4)}$$

Where, σ is the standard deviation of blank measurement[3] and k is the slope between fluorescence intensity versus respective metal ion concentration. Standard deviation is calculated from of free UiO-66-NH-PTCDA-Na measured its fluorescence intensity with five times and shows standard deviation of 114.1316.

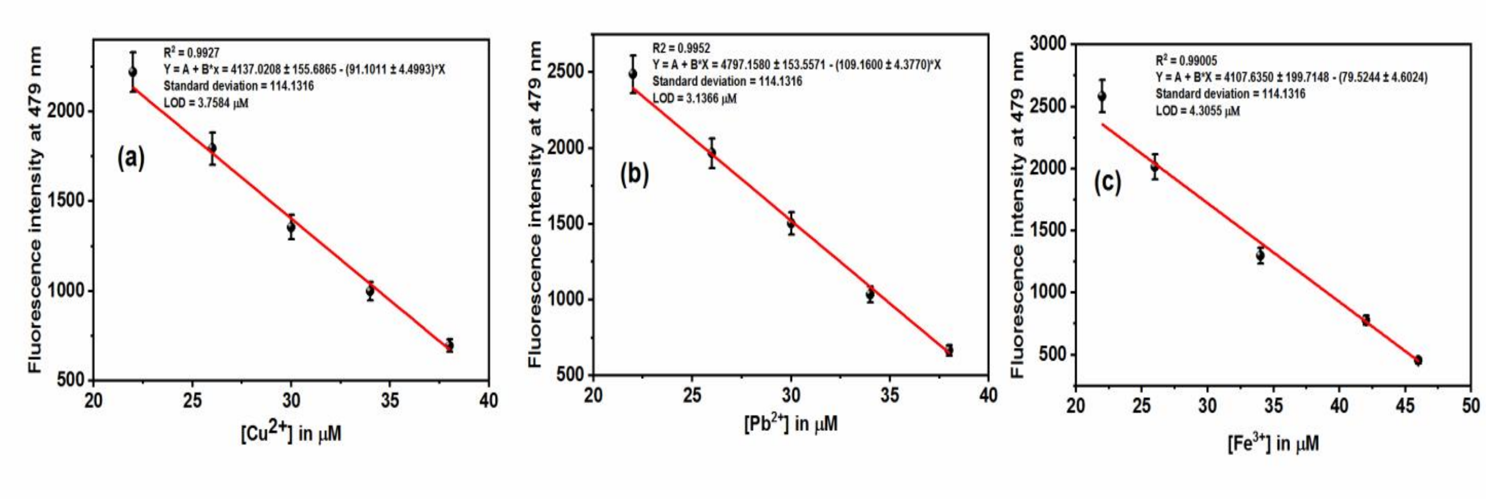

Fig. S10 Determination of LOD (a) Linear regressive plot of UiO-66-NH-PTCDA-Na with Cu^{2+} ion concentration (b) Linear regressive plot of UiO-66-NH-PTCDA-Na with Pb^{2+} ion concentration (c) Linear regressive plot of UiO-66-NH-PTCDA-Na with Fe^{3+} ion concentration.

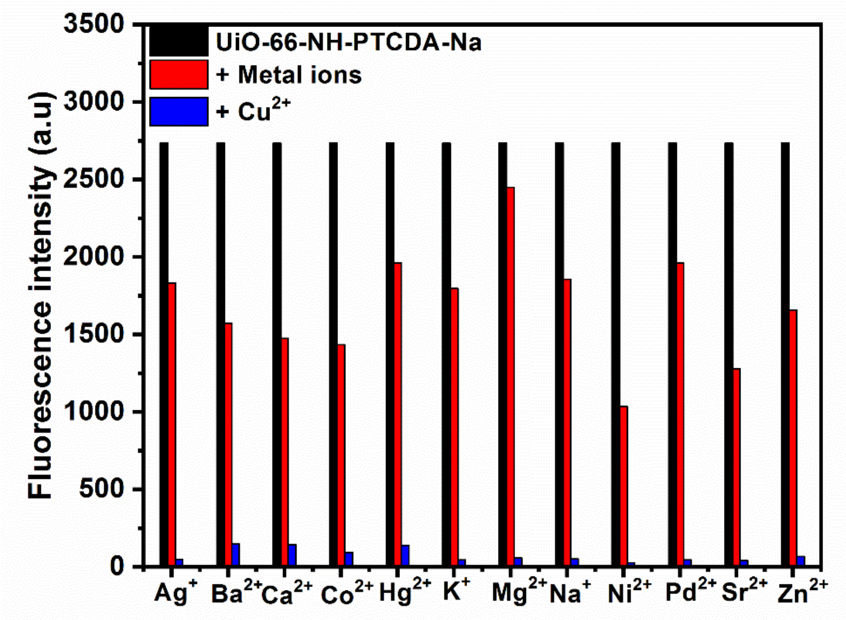

Fig. S11. Fluorescence interference study of UiO-66-NH-PTCDA-Na in the presence of competitive metal ions (1 equiv.) with and without Cu^{2+} ions (1.0 equiv.).

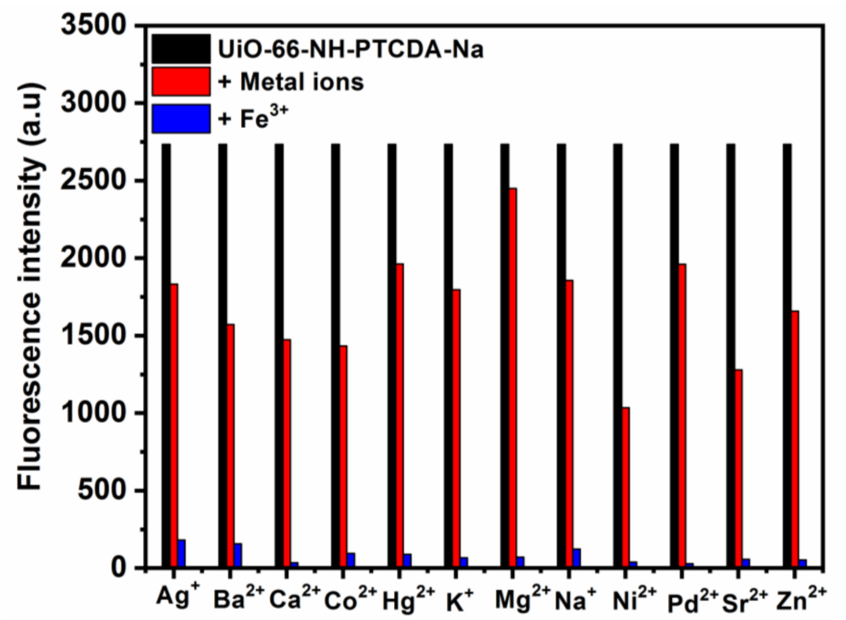

Fig. S12. Fluorescence interference study of UiO-66-NH-PTCDA-Na in the presence of competitive metal ions (1 equiv.) with and without Fe^{3+} ions (1.0 equiv.).

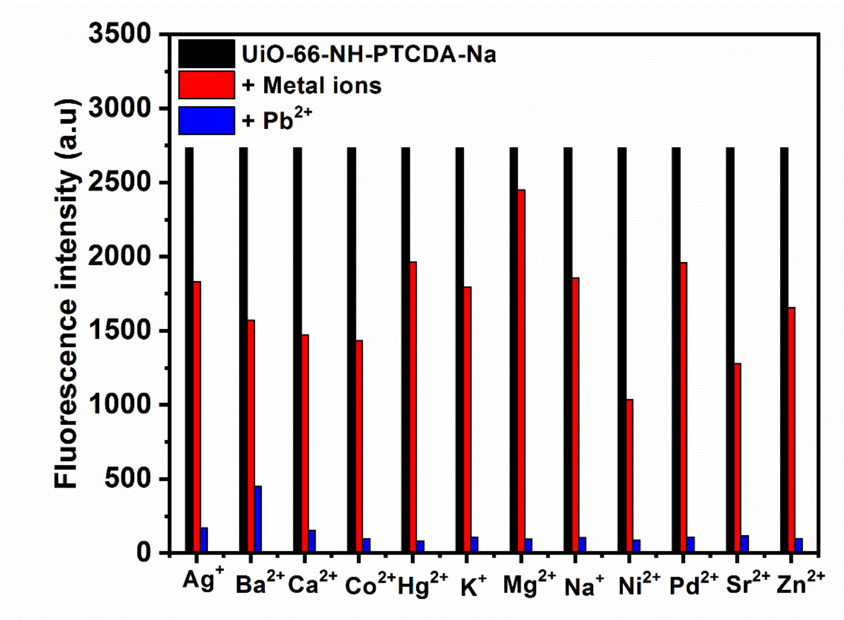

Fig. S13. Fluorescence interference study of UiO-66-NH-PTCDA-Na in the presence of competitive metal ions (1 equiv.) with and without Pb^{2+} ions (1.0 equiv.).

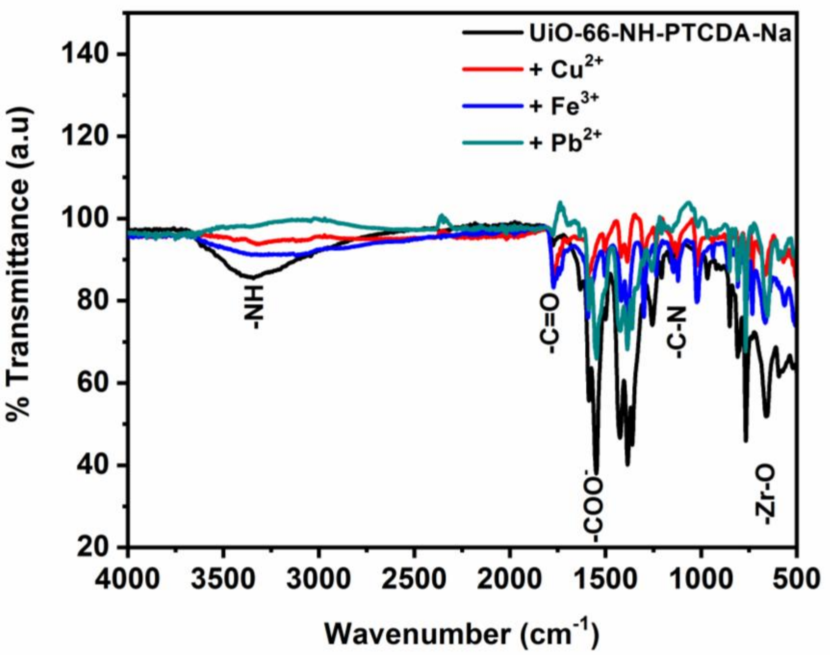

Fig. S14. FT-IR spectra of UiO-66-NH-PTCDA-Na in the presence and absence of sensing metal ions (Cu^{2+}, Fe^{3+} & Pb^{2+}).

Table S2. Comparison of fluorescence sensing performance of UiO-66-NH_2 based MOFs with literature.

S. No	MOF Sensors	Analytes	Sensing medium	LOD (µM)	Reference
1	UiO-66-NH_2-IM	Fe^{3+} and CO_3^{2-}	Aqueous	0.67 and 1.16	4
2	LTP @ UiO-66-NH_2	U^{6+}	Aqueous	0.08	5
3	UiO-66-HN	Formaldehyde	PBS buffer-DMSO	0.167	6
4	UiO-66-N=CH_2	Cd^{2+}	Aqueous	0.336	7
5	Eu^{3+}/Cu^{2+}@UiO-66-$(COOH)_2$	H_2S	HEPES buffer	5.45	8
6	UiO-66-MA	H_2S and Cu^{2+}	Aqueous	0.0033 and 0.0026	9
7	UiO-66-NH_2	F^-, $H_2PO_4^-$ and TNP	Aqueous	0.82, 0.73 and 0.21	10
8	Zr based MFCs	Zn^{2+}	Aqueous	0.00857	11
9	UiO-66-NH_2-DHB	Fe^{3+}	Aqueous	0.58	12
10	TCPP@UiO-66-NH_2	Cu^{2+}	Aqueous	0.024	13
11	UiO-66-NH_2@TA	Pb^{2+}	Aqueous	0.18	14
12	**UiO-66-NH-PTCDA-Na**	**Cu^{2+}, Fe^{3+} & Pb^{2+} ions**	**(HEPES buffer (pH = 7.0))**	**3.75, 4.30, and 3.13**	**This work**

References

1 P. Makuła, M. Pacia and W. Macyk, *J. Phys. Chem. Lett.*, 2018, **9**, 6814–6817.
2 K. Fabrizio, K. N. Le, A. B. Andreeva, C. H. Hendon and C. K. Brozek, *ACS Mater. Lett.*, 2022, **4**, 457–463.
3 K. A. Karthick, B. Shankar, S. Gayathri, M. K. Aravind, B. Ashokkumar and A. Tamilselvi, *New J. Chem.*, 2023, **47**, 9427–9439.
4 D. P. Biswal, D. Singha, J. Panda and M. Kumar Rana, *ChemPhysChem*, 2023, **24**, e202300311.
5 J. Liu, X. Wang, Y. Zhao, Y. Xu, Y. Pan, S. Feng, J. Liu, X. Huang and H. Wang, *Anal. Chem.,* 2022, **94**, 10091–10100.
6 X. Li, H. Qu, Y. Wang, X. Zhang, L. Bai and Z. Wang, *J. Solid State Chem.*, 2023, **317**, 123672.
7 J. Wang, T. Xia, X. Zhang, Q. Zhang, Y. Cui, Y. Yang and G. Qian, *RSC Adv.*, 2017, **7**, 54892–54897.
8 X. Zhang, Q. Hu, T. Xia, J. Zhang, Y. Yang, Y. Cui, B. Chen and G. Qian, *ACS Appl. Mater. Interfaces*, 2016, **8**, 32259–32265.
9 X.-L. Yang, C. Ding, R.-F. Guan, W.-H. Zhang, Y. Feng and M.-H. Xie, *J. Hazard. Mater.*, 2021, **403**, 123698.
10 R. Dalapati and S. Biswas, *Sens. Actuators B: Chem.*, 2017, **239**, 759–767.
11 I. M. El-Sewify, M. A. Shenashen, A. Shahat, M. M. Selim, M. M. H. Khalil and S. A. El-Safty, *Microchem. J.*, 2018, **139**, 24–33.
12 A. G. Achumi, M. Pamei and A. Puzari, *Inorg. Chem. Commun.*, 2025, **179**, 114794.
13 J. Du, D. Lin, W. Chen, Q. Sun and E. Gao, *CrystEngComm*, 2025, **27**, 488–496.
14 K. Wang, X. Duan, Y. Tian, H. Lin, L. Cao and J. Sui, *Spectrochim. Acta Part B: At. Spectrosc.*, 2025, **225**, 107120.